Glycoconjugate Journal (1997) **14:** 729–736

β-Galactosidase-deficient mouse as an animal model for G_{M1}-gangliosidosis

Junichiro Matsuda[1]*, Osamu Suzuki[1], Akihiro Oshima[1], Atsuo Ogura[1], Yoko Noguchi[1], Yoshie Yamamoto[1], Toshihiko Asano[2], Kazuhiro Takimoto[2], Kazuko Sukegawa[3], Yoshiyuki Suzuki[4] and Masaharu Naiki[1†]

[1]*Department of Veterinary Science and* [2]*Division of Experimental Animal Research, National Institute of Health, 1-23-1 Toyama, Shinjuku-ku, Tokyo 162, Japan*
[3]*Department of Pediatrics, School of Medicine, Gifu University, 40 Tsukasa-machi, Gifu 500, Japan*
[4]*The Tokyo Metropolitan Institute of Medical Science, 3-18-22 Honkomagome, Bunkyo-ku, Tokyo 113, Japan*

G_{M1}-gangliosidosis is a progressive neurological disease in humans caused by deficiency of lysosomal acid β-galactosidase, which hydrolyses the terminal β-galactosidic residue from ganglioside G_{M1} and other glycoconjugates. In this study, we generated a mouse model for G_{M1}-gangliosidosis by gene targeting in embryonic stem cells. The mouse homozygous for the disrupted β-galactosidase gene showed β-galactosidase deficiency, presented with progressive spastic diplegia, and died of emaciation at 7–10 months of age. Pathologically, PAS-positive intracytoplasmic storage was observed in neuronal cells of various areas in the brain. Biochemical analysis revealed a marked accumulation of ganglioside G_{M1} and asialo G_{M1} in brain tissue. This animal model will be useful for pathogenetic analysis and therapeutic trial of human G_{M1}-gangliosidosis.

***Keywords*: G_{M1}-gangliosidosis, β-galactosidase, gene targeting, lysosomal storage diseases, disease models, animal**

Introduction

G_{M1}-gangliosidosis is a progressive neurological disease in humans caused by hereditary deficiency of lysosomal acid β-galactosidase that hydrolyses the terminal β-galactosidic residue of ganglioside G_{M1} and other glycoconjugates [1]. Numerous β-galactosidase gene mutations have been identified in the clinical forms of infantile, juvenile, and adult onset [2]. Another type of human β-galactosidase deficiency (Morquio B disease), presenting clinically with generalized skeletal dysplasia, is caused by mutations of the same gene but different from those for G_{M1}-gangliosidosis [3]. The pathogenesis of these diverse phenotypic expressions is not yet known.

Although animal models have been reported in some species, such as cats [4], dogs [5], sheep [6] and calves [7], a mouse model for conventional laboratory use has not yet been reported. In this study, we generated a mouse model for G_{M1}-gangliosidosis with the β-galactosidase gene disrupted by homologous recombination in embryonic stem (ES) cells. These mice showed a progressive neurological disease, β-galactosidase deficiency, cerebral storage of ganglioside G_{M1}, and widespread cerebral lesions with intraneuronal storage of membranous cytoplasmic bodies. They died of emaciation and malnutrition at 7–10 months of age. We concluded that this mouse is an authentic model of human G_{M1}-gangliosidosis.

Methods

Construction of targeting vector

For disruption of the mouse β-galactosidase gene, a displacement-type targeting vector [8] was constructed. The genomic clones of murine β-galactosidase were isolated from a genomic DNA library of TT2 ES cells derived from C57BL/6 × CBA F1 male mice [9, 10], using murine β-galactosidase cDNA [11] as a probe. The 5 kb *Hin*dIII fragment containing exon 15 of the gene was subcloned into pHSV-106 (herpes simplex virus thymidine kinase gene containing vector, GIBCO/BRL Life Technologies, USA), in which the *Sal*I site was previously destroyed by blunting. A neo resistance cassette (1.1 kb *Xho*I-*Sal*I fragment) from pMC1 neo polyA (Stratagene, USA) was inserted into the *Sal*I site in exon 15, to disrupt the coding sequence of the gene. The resulting plasmid was linearized by *Cla*I digestion. The construct of the targeting vector is illustrated in Figure 1A.

*To whom correspondence should be addressed.
Tel: +81-3-5285-1111; Fax: +81-3-5285-1179.
† Deceased on 26 December 1996.

0282–0080

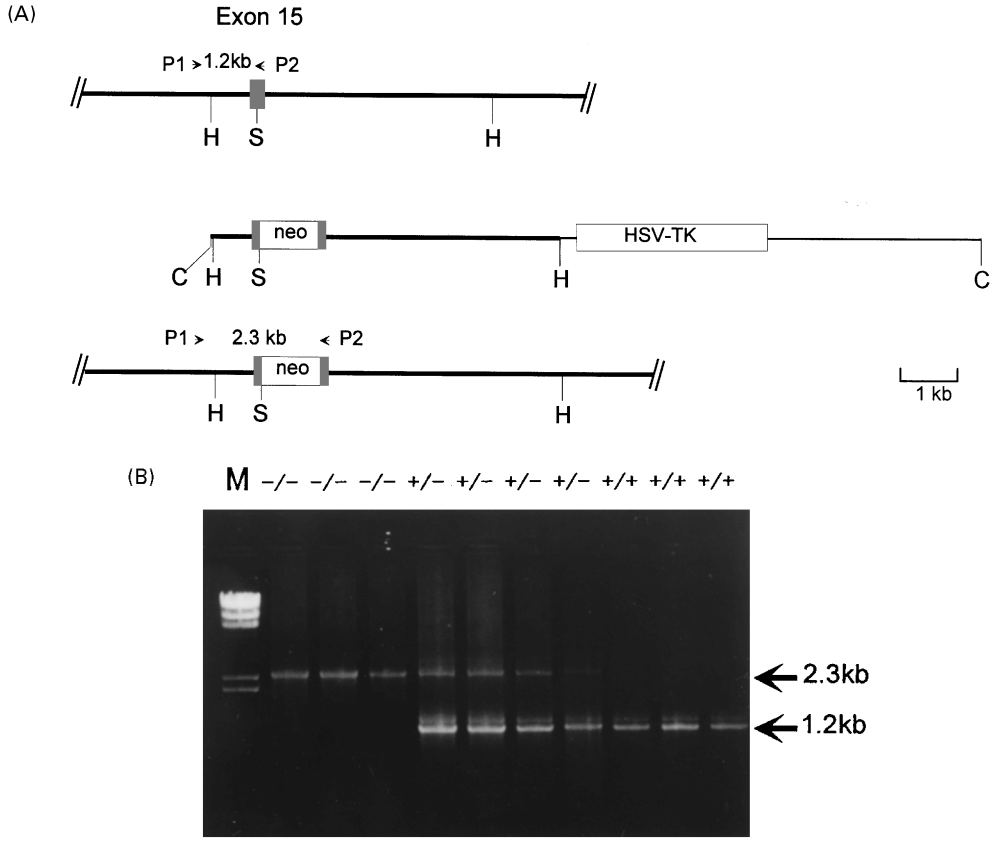

Figure 1. Strategy for disruption of the murine β-galactosidase gene. (A) Schematic representation of the normal murine β-galactosidase genomic fragment including exon 15 (*top*), the targeting vector (*middle*) and the targeted gene (*bottom*). Exon 15 is shown as a box, and introns as lines. The targeting vector has a neomycin resistance cassette (neo) inserted into exon 15 at the *Sal*I site, and a herpes simplex virus thymidine kinase cassette (HSV-TK) at its 3′ end. Arrows indicate locations of the primers (P1, P2) used for genotyping by PCR. H, *Hin*dIII; S, *Sal*I; C, *Cla*I. (B) Genotyping of normal (+/+), heterozygous (+/−) and homozygous mutant (−/−) mice by PCR. M, molecular weight marker (λ/*Hin*dIII digest).

Gene targeting in ES cells

TT2 ES cells were cultured on mitomycin C-treated primary embryonic fibroblasts from the ICR fetus as a feeder layer in a 6 cm dish, in Dulbecco's modified Eagle MEM (high glucose, no pyruvate; GIBCO/BRL) supplemented with 20% fetal bovine serum, 0.1 mM 2-mercaptoethanol, MEM non-essential amino acid solution (GIBCO/BRL), five nucleosides [12], and 1000 IU ml^{-1} of leukemia inhibitory factor [13] (AMRAD, Australia). Approximately 3×10^7 TT2 cells and 25 μg of linearized vector were suspended in a medium, containing 20 mM HEPES, 137 mM NaCl, 5 mM KCl, 0.7 mM $Na_2HPO_4 \times 12H_2O$, 6 mM glucose, 0.1 mM 2-mercaptoethanol [14], and the cells were electrophorated at 250 V, 960 μF using a Gene Pulser (Bio-Rad, USA). They were then suspended in 100 ml of the medium, and seeded on ten 10 cm dishes preseeded with mitomycin C-treated STO cells that had been transfected with and were continuously expressing the neoresistance gene (pMC1neo polyA). The culture medium was changed daily.

G418 (450 μg ml^{-1}; GIBCO) was added to the medium 2 days after the transfection, and, in addition, ganciclovir (2 μM; gift of Roche Bioscience, USA) was added 3 days after the transfection. The ES cell colonies resistant to both drugs were chosen 10 days after transfection, and each was seeded on a 24-well dish preseeded with mitomycin C-treated primary fibroblasts. Two days later, one half of the cells in each well were expanded into 6-well dishes with feeder cells. The other half were checked for the occurrence of gene targeting events by PCR and Southern blotting. Two days later, the homologous recombinant clones as identified above were expanded on 6 cm dishes with a feeder layer without freezing-thawing before production of chimeric mice.

Generation of knockout mouse and confirmation of gene disruption

Chimeric mice were produced as described [9]. Three targeted ES cell clones (2A6, 3D1 and 1B6) were used for

chimera production. About 10–15 ES cells were microinjected into the perivitelline space of ICR 8-cell embryos, and the injected embryos were cultured overnight to develop into morulae stage. Then the embryos were transferred into uteri of pseudopregnant ICR females. Three chimera males from the 3D1 clone were identified as germline chimeras by test breeding with ICR females. Coloured (black and agouti) offspring of chimeric mice and ICR females were analysed by PCR amplification of neoresistance gene for transmission of the mutant allele. Homozygotes for the disrupted β-galactosidase gene were generated by mating heterozygotes. Genotypes of the progenies were determined by PCR amplification of DNA from tail or liver, using the sense primer P1 (5′-GTGGACCCTGTATCACCCCATCTTACT-3′) and the antisense primer P2 (5′-CTTGGACCACCCAGGAAACTGGATGAA-3′) for detection of a 1.2 kb band for the wild-type allele and 2.3 kb band for the mutant allele. PCR was performed using *Taq* polymerase (GIBCO BRL) at 35 cycles of reaction at 94 °C for 1 min, at 58 °C for 1 min and at 72 °C for 3 min.

Pathology

For light microscopy, the brain was fixed with buffered formalin and embedded in paraffin. Sections of 4 μm thickness were stained with Nissl's stain. Frozen sections were stained with the periodic acid-Schiff (PAS) method. For electron microscopy, a small piece of the brain was fixed with 2.5% glutaraldehyde in 0.1% cacodylate buffer, postfixed with 1% osmium tetroxide and embedded in a mixture of Araldite and epoxy-resin. Ultrathin sections of 60 nm thickness were stained with uranyl acetate and lead citrate.

Biochemistry

The enzyme activity was assayed with 4-methylumbelliferyl β-D-galactoside (Nacalai Tesque, Japan) as a substrate, as described previously [15]. The protein concentration was determined by the method of Bradford [16].

Glycolipids in brain and liver were analysed. The brain was roughly divided into three regions: cerebral hemisphere, brain stem, and cerebellum. The ganglioside fractions were obtained by the Folch extraction and partition of total lipids [17], and the pooled upper phase was saponified with 0.5 ml of 0.2 N KOH/methanol and desalted with Sep-Pak C18 reverse-phase cartridge [18] (Waters, USA). Individual gangliosides were separated by high performance thin-layer chromatography (HPTLC) on a plate precoated with super fine silica gel 60 (E. Merck, Germany), with chloroform : methanol : 0.2% $CaCl_2$ (60 : 35 : 8, by vol) for development, and visualized with resorcinol reagent for qualitative and quantitative analysis [19]. Neutral glycosphingolipids (GSLs) were isolated from the lower phase of the Folch partition. The fraction was acetylated with pyridine-acetic anhydride (3 : 1, by vol), and acetylated GSLs were purified by Sep-Pak Florisil cartridge (Waters) chromatography using acetone-dichloroethane (1 : 1, by vol) as an elution solvent according to Saito and Hakomori [20]. For deacetylation, the acetylated GSLs were saponified as described in the ganglioside purification procedure. Individual neutral GSLs were separated by HPTLC with chloroform : methanol : 0.2% $CaCl_2$ (60 : 25 : 4, by vol) for development and anthrone reagent for visualization [21].

Urinary oligosaccharide patterns in mutant and normal mice, and an infantile G_{M1}-gangliosidosis patient were determined. Urine samples (800–1500 μl) corresponding to 1 mg creatinine were centrifuged at 1500 × **g** for 10 min and the supernatants were desalted by Dowex 50-X8/Dowex 1-X8. Desalted urines were lyophilized and resuspended in 50 μl deionized water, then an aliquot (10 μl) of each sample was applied to TLC plates and chromatographed as previously reported by Sewell [22].

For the analysis of urinary glycosaminoglycans (GAGs), the GAGs precipitated with cetylpyridinium chloride were electrophoresed on a cellulose acetate plate as described previously [23]. Liver keratan sulfates were isolated by the method of Callahan and Wolfe [24], and analysed by electrophoresis.

Results

Confirmation of gene disruption

Out of 258 G418/ganciclovir resistant colonies, three were identified as homologous recombinants. The cells from these targeted colonies were injected into eight-cell embryos of ICR mice to produce chimeras. Chimeric males were mated to ICR female mice, and three chimeric males derived from one ES cell colony were found to have transmitted the β-galactosidase mutation to their progeny. But no chimeric male derived from the other two ES cell colonies gave birth to mice with the mutant allele. The heterozygous mouse pairs were mated to generate homozygous progeny (β-Galactosidase knockout mouse). Genotyping of these mice by PCR is shown in Figure 1B. β-Galactosidase activity in the tail of the mice, with 4-methylumbelliferyl β-galactoside as a substrate, was extremely low in homozygous mutants (average 6.8% and range 0–10% of the wild-type mean), and half normal in heterozygotes (Figure 2A). These data indicated that targeted disruption of the β-galactosidase gene was successfully achieved.

Clinical manifestations

Summary of neurological manifestations of mutant mice was already described elsewhere [25]. Homozygous mutants were born normally, and were apparently healthy at least until 4 months of age. Then, their locomotor activities gradually decreased. Horizontal movements were slow, and rearing or vertical climbing became less frequent. By 6–8 months, they exhibited definite gait disturbance with mild

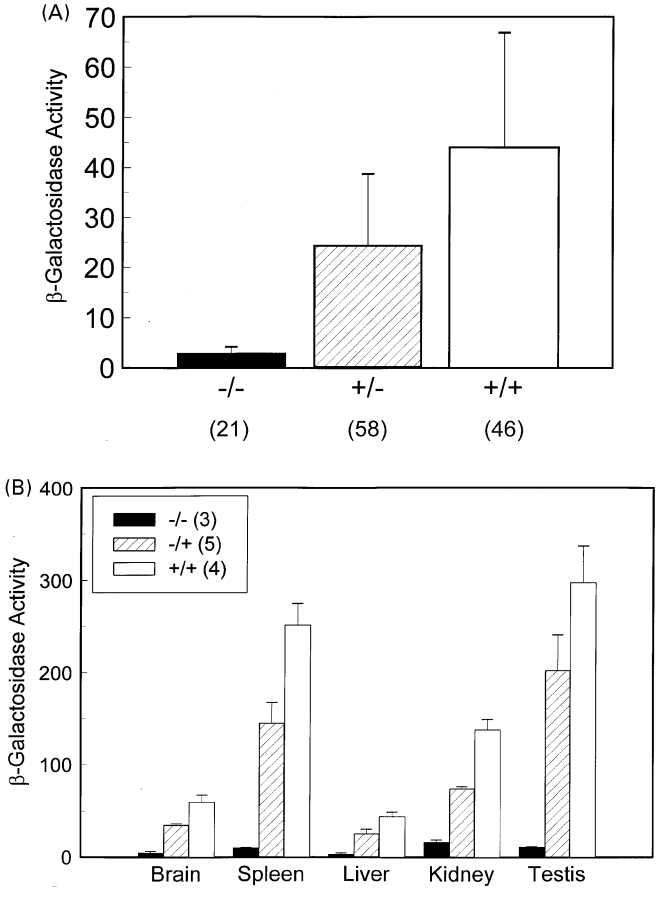

Figure 2. β-Galactosidase activities in mouse tissues. (A) tail; (B) other tissues from normal (+/+), heterozygous (+/–) and homozygous mutant (–/–) mice. Activities were assayed with 4-methylumbelliferyl β-D-galactoside as a substrate and expressed as nmol mg^{-1} protein h^{-1}. Each value is indicated as mean $\pm$ SD, and the number of animals is shown in parentheses.

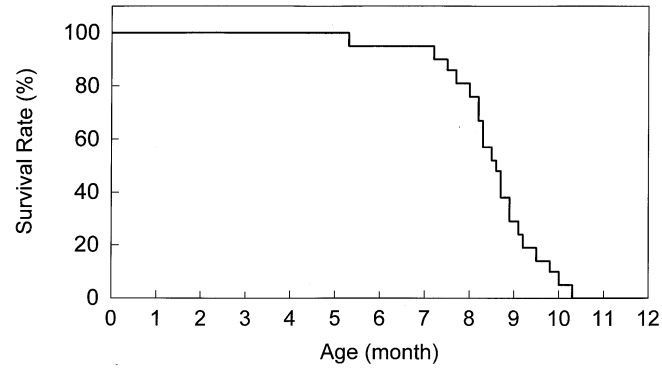

Figure 3. Survival curve of the β-galactosidase knockout mouse. Survival rates (%) of 21 knockout mice at F2 generation are plotted for 12 months after birth. All heterozygous and wild type litter mates of these knockout mice survived at least until 12 months of age.

shaking. They often tottered, with forelimbs flexed, hindlimbs extended and extroverted, and tail straightly raised upward. When hung vertically with the tail held upward, they huddled themselves with all four limbs flexed [25]. Normal mice always extended their limbs in this downward vertical position. This abnormal posture appeared first with hindlimbs, and then gradually spread to forelimbs with the progress of the disease. At the terminal stage, body movements were associated with shaking, and generalized and progressive paralysis appeared. Finally they became emaciated because of difficulty feeding. They died at 7–10 months of age (Figure 3). The life span was 254.4 ± 30.5 days (mean $\pm$ SD, $n = 21$) in the knockout group. The body weight at death was less than half of normal or heterozygous littermates. Heterozygous mice exhibited no obvious abnormality. Reproductive performance of F2 homozygous mutants was abnormal, with a relatively higher incidence of sterility and cannibalism. However, about a half of homozygote pairs could produce at least one litter before they developed the symptoms described above. The knockout homozygotes have been successfully maintained to the F6 generation up to the present.

Pathology

Unlike the human disease infants, hepatosplenomegaly was not observed; the sizes of liver and spleen were smaller than those in normal control mice. Vacuolated lymphocytes were almost always observed in the peripheral blood. Skeletal dysplasia was not evident. Brain was normal in size and weight. However, numerous neurons were degenerated with distended cytoplasm histopathologically in various areas of the central nervous system, such as cerebral cortex, basal ganglia, thalamus, and hypothalamus (Figure 4A). Pons and medulla oblongata also were affected. Purkinje cells were specifically affected in cerebellum. The distended neuronal cytoplasm was strongly positive for PAS stain in frozen sections. Electron microscopy demonstrated multilamellar and myelin-like inclusion bodies (membranous cytoplasmic bodies; MCBs) in neuronal cytoplasm (Figure 4C), like those reported in human G_{M1}-gangliosidosis [26].

Biochemistry

In all organs examined, mutant homozygotes showed β-galactosidase deficiency (Figure 2B). The activity was extremely low in the brain. Relatively high residual activities were observed in the spleen, testes and kidneys under the present assay conditions with an artificial substrate. In these organs, normal mice also showed relatively high activities as compared with brain activity. Heterozygotes showed intermediate activities between normal and mutant homozygotes. In addition, primary embryonic fibroblasts were isolated from mutant and normal fetuses and their enzyme activities were assayed. Essentially no detectable activity was observed in the mutant fibroblasts (0–1% of normal).

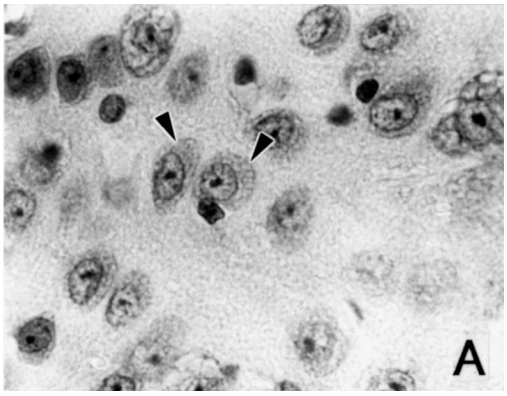

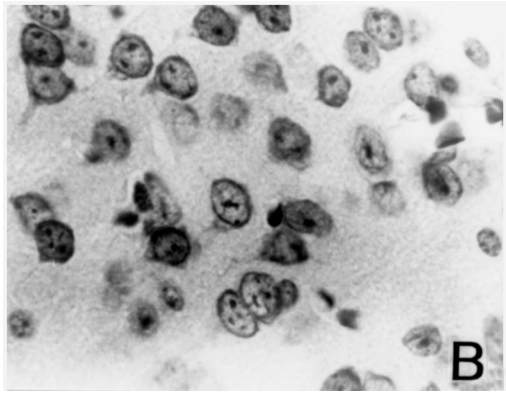

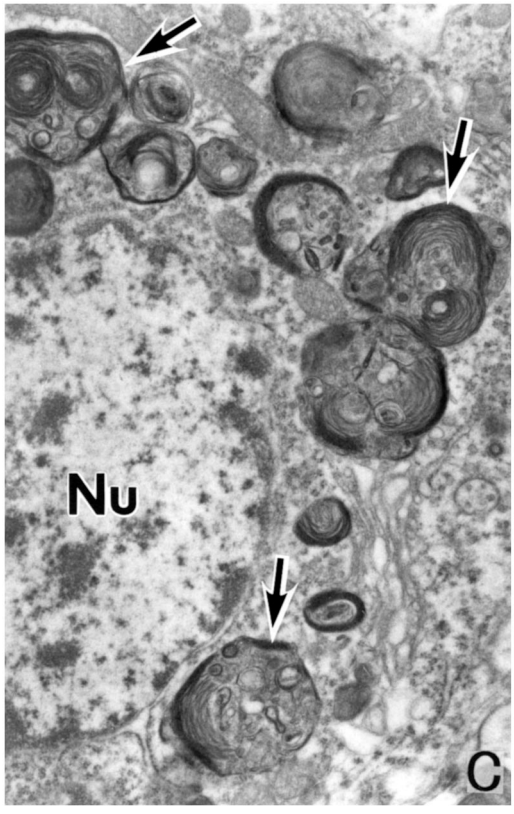

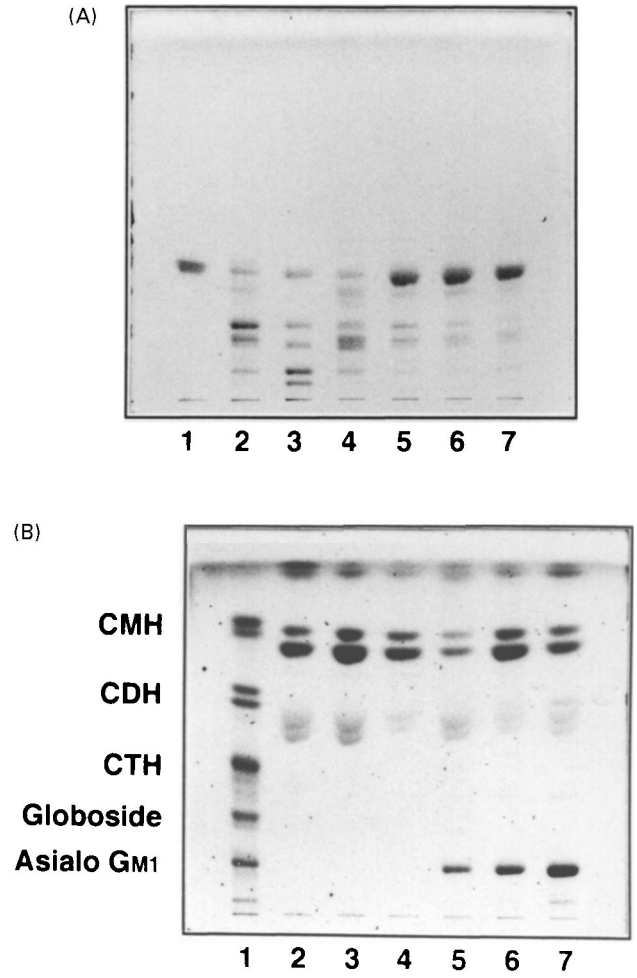

Figure 5. HPTLC of gangliosides (A) and neutral glycosphingolipids (B) in brain. (A) Approximately 1.5 μg lipid-bound sialic acid were spotted for each sample. The gangliosides were developed with chloroform : methanol : 0.2% $CaCl_2$ (60 : 35 : 8, by vol), and visualized with resorcinol-HCl reagent. Lane 1, G_{M1} standard; lane 2: cerebrum of a normal mouse; lane 3, brain stem of a normal mouse; lane 4, cerebellum of a normal mouse; lane 5, cerebrum of a mutant mouse; lane 6, brain stem of a mutant mouse; lane 7, cerebellum of a mutant mouse. (B) Neutral glycosphingolipids corresponding to 1 mg of dry tissue were spotted for each sample, developed with chloroform : methanol : 0.2% $CaCl_2$ (60 : 25 : 4, by vol), and then visualized with anthrone-H_2SO_4. Lane 1, standard samples, asialo G_{M1}; globoside; CTH, trihexosylceramide; CDH, lactosylceramide; CMH, glucosylceramide; lanes 2–7, same samples as above. All samples are from 6-month-old mice at F2 generation.

Figure 4. Pathological changes of the brain in the *β*-galactosidase knockout mouse. Light microscopy of cerebrum in a homozygous mutant mouse (A) and a normal mouse (B); ×250. Nissl-stained sections. Distended cytoplasm with large vacuoles is noted in the mutant mouse (arrowheads). (C) Electron microscopy of a Purkinje cell in the mutant mouse; ×14 000. MCBs at various stage of development are observed in the cytoplasm (arrows). Nu, nucleus. All sections are from 6 month-old mice at F2 generation.

HPTLC analysis showed that the ganglioside G_{M1} content was markedly increased in all three brain regions of the mutant mice as compared to that in normal brain (Figure 5A). G_{M1} accounted for 70% of total lipid-bound sialic acid (normal controls 12–18%), resulting in four- to six-fold increase in relative amount. Furthermore, the total ganglioside was increased three- to four-fold. Taken together, the amount of G_{M1} was calculated to be increased about 20-fold in the brain of the mutant mouse. Asialo G_{M1} (G_{A1}) was also increased as much as G_{M1} in mutant mouse brain, whereas G_{A1} was not detected in normal brain (Figure 5B). In addition, remarkable accumulation of both G_{M1} and G_{A1} was detected in mutant mouse liver (Figure 6A and B).

The analysis of urinary oligosaccharides by TLC showed that abnormal oligosaccharide bands were observed in mutant mice, but not in normal mice. The abnormal chromatographic pattern in mutant mice was similar to that of a G_{M1}-gangliosidosis patient (Figure 7). The analysis of urinary GAGs revealed there was no marked difference between mutant and normal mice. Furthermore, keratan sulfate was undetectable in urine both from mutant and normal mice (data not shown). In addition, only trace levels of keratan sulfate were detected both in mutant and normal mouse livers (data not shown).

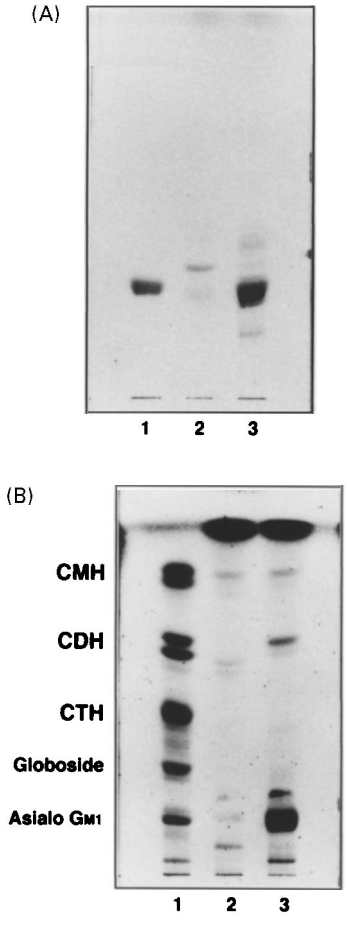

Figure 6. HPTLC of gangliosides (A) and neutral glycosphingolipids (B) in liver. (A) Gangliosides corresponding to 10 mg of dried liver tissue of mutant mouse and 20 mg of normal mouse were spotted. HPTLC was carried out as described in Figure 5. Lane 1, G_{M1} standard; lane 2, liver of a normal mouse; lane 3, liver of a mutant mouse. (B) Neutral glycosphingolipids corresponding to 10 mg of dry tissue of mutant mouse and 20 mg of a normal mouse were spotted. HPTLC was carried out as described in Figure 5. Lane 1, standard samples same as Figure 5B; lane 2, normal mouse; lane 3, mutant mouse. All samples are from 6 month-old mice at F2 generation.

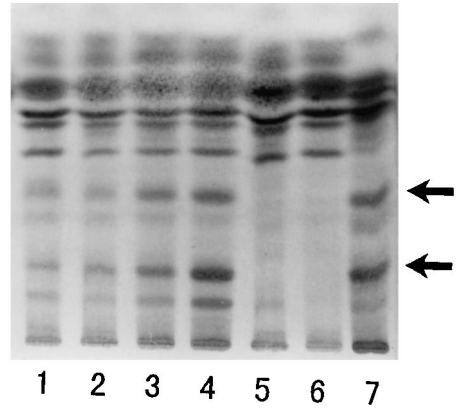

Figure 7. TLC of oligosaccharides in urine. Lanes 1, 2, mutant male mice; lanes 3 and 4, mutant female mice; lane 5, normal male mouse; lane 6, normal female mouse; lane 7, human G_{M1}-gangliosidosis patient. Arrows indicate typical abnormal bands observed both in mutant mice and a human patient.

Discussion

From these data described above, we concluded that the β-galactosidase gene-disrupted mouse showed biochemical, morphological, and clinical similarities to human G_{M1}-gangliosidosis. There is a genetic variation of β-galactosidase activity among various mouse strains [27]. Particularly in the DBA/2 mouse strain, a low enzyme activity and a high concentration of brain ganglioside G_{M1} were described [28]. However, this strain does not develop any clinical manifestations that have been observed in human G_{M1}-gangliosidosis. Although there was a wide individual variation, the residual activity appeared relatively high in some organs of the gene-disrupted mice in this study. In contrast, no detectable activity was observed in mutant embryonic fibroblasts. The reason for these differences in residual activity among various tissues is not known. Concomitant neutral β-galactosidase may have contributed to relatively high residual activity under our assay conditions. In this study, all enzyme assays were performed with an artificial substrate, and we need to use a natural substrate like ganglioside G_{M1} for evaluation of actual intracellular activity of the enzyme in these disease animals.

It is noteworthy that G_{A1} accumulated as much as G_{M1} in the mutant mouse brain and liver. On the other hand, in

human G_{M1}-gangliosidosis, storage of G_{A1} is less prominent compared with the remarkable storage of G_{M1} [29]. Recently, Sango *et al.* [30] reported that in the case of a mouse model of Sandhoff disease, in which both β-hexosaminidase A and B were deficient, asialo G_{M2} as well as G_{M2} extensively accumulated in brain. They suggested that mouse sialidase(s) could convert a significant amount of G_{M2} to asialo G_{M2}. Similarly, in the G_{M1}-gangliosidosis mouse, it could be possible that G_{M1} is converted to G_{A1} by mouse sialidase(s). These assumptions are also supported by the observation of sialidase activity which can convert G_{M1} to G_{A1} and G_{M2} to asialo G_{M2} in mouse Neuro2a cells [31].

Accumulation of keratan sulfate in liver and its increased excretion in urine are characteristic of Morquio B disease and infantile and juvenile G_{M1}-gangliosidosis. However, keratan sulfate was not detected either in normal or mutant mouse urine, and furthermore keratan sulfate was basically absent in livers of both normal and mutant mice. It has been reported that the mouse does not synthesize skeletal keratan sulfate, even though corneal keratan sulfate is synthesized [32]. Therefore the absence of keratan sulfate in mutant mouse urine could be due to the lack of keratan sulfate synthesis in almost all tissues except cornea. In addition, there were no obvious abnormalities in the skeletal system of mutant mice. This again might be explained by the absence of skeletal keratan sulfate in mice. Various kinds of oligosaccharides with β-galactosidic linkage at the non-reducing end, which are derived from glycoproteins, have been detected in G_{M1}-gangliosidosis [33]. In urine from the homozygous mutant mouse, an abnormal oligosaccharide pattern resembling that in human G_{M1}-gangliosidosis was detected by TLC analysis. These data again support our findings that this mouse is a murine counterpart of human G_{M1}-gangliosidosis, apparently without keratan sulfaturia or bone dysplasias characteristic of Morquio B disease.

In human β-galactosidase-deficient disorders, phenotypic expressions are diverse, and therefore classified clinically into two major subgroups; G_{M1}-gangliosidosis presenting predominantly with the central nervous system manifestations, and Morquio B disease presenting with systemic bone dysplasia, without nervous system involvement [1]. Furthermore, G_{M1}-gangliosidosis is classified into infantile, juvenile and adult forms on the basis of the age of onset and severity of the disease. In Table 1, clinical, pathological and biochemical aspects of human and murine diseases are summarized and compared with one another. This disease model mouse seems to be clinically similar to the infantile or juvenile form of human G_{M1}-gangliosidosis, although there are some dissimilarities with both of them. For comparison of the disease in two different species, the time course of ontogeny should be taken into consideration. Gestation lasts 40 weeks in humans, and 3 weeks in mice. On the other hand, postnatal maturation lasts 10–15 years before acquiring fertility in humans, and 2 months in mice. These time factors may affect evolution of a genetically determined disease like hereditary β-galactosidase deficiency.

Some model animals have been reported for G_{M1}-gangliosidosis [4–7]. However, those animals reported until now have not often been used for conventional research experiments, because of their large size, long life span, and difficulty of handling in a clinical or basic research laboratory. For these reasons, our model mouse has a definite advantage for genetic and biochemical analysis, with short life span, fertility even between mutant homozygotes, and development of clinically observable neurological manifestations that rapidly progress to death within a few months after the onset.

This β-galactosidase-deficient mouse will therefore provide more information about the pathogenesis and treatment of the human inherited diseases represented by G_{M1}-gangliosidosis. Biochemical and cell/tissue biological analysis on this particular experimental animal may disclose the pathogenesis of clinical and pathological heterogeneity in human β-galactosidase deficiency. Furthermore, this model mouse in particularly useful for evaluation of molecular

Table 1. Comparison of human and murine G_{M1}-gangliosidoses.

	Infantile[a]	*Juvenile*[a]	*Adult/chronic*[a]	*Murine*
Onset	0–6 mo	7 mo–3 yr	3–30 yr	4 mo
Hepatosplenomegaly	+	+or −	–	–
Vacuolated lymphocytes	+	+	+or −	+
CNS pathology[b]	Generalized	Generalized	Localized[c]	Generalized
Skeletal dysplasia	Generalized	Localized[d]	Localized[d]	None (?)
G_{M1} storage	+++	++	+	+++
β-Galactosidase activity[e]	0–2%	2–3%	3–7%	0–1%

[a]Human disease.
[b]CNS: central nervous system.
[c]Extrapyramidal system.
[d]Vertebral deformity.
[e]Source: cultured fibroblasts, substrate: 4-methylumbelliferyl β-galactoside.

therapeutic effects on the central nervous system, because the neurological manifestations are easily recognizable clinically and pathologically.

Acknowledgements

This work was supported by grants from the Ministry of Education, Science, Sports and Culture of Japan, the Ministry of Health and Welfare of Japan, Japan Health Sciences Foundation, and Yamanouchi Foundation for Research on Metabolic Disorders.

References

1 Suzuki Y, Sakuraba H, Oshima A (1995) In *The Metabolic and Molecular Bases of Inherited Disease*, 7th edition (Scriver CR, Beaudet AL, Sly WS, Valle D, eds) pp 2785–824. New York: McGraw-Hill, Inc.
2 Yoshida K, Oshima A, Shimmoto M, Fukuhara Y, Sakuraba H, Suzuki Y (1991) *Am J Hum Genet* **49**: 435–42.
3 Oshima A, Yoshida K, Shimmoto M, Fukuhara Y, Sakuraba H, Suzuki Y (1991) *Am J Hum Genet* **49**: 1091–93.
4 Baker HJJ, Lindsey JR, McKhann GM, Farrell DF (1971) *Science* **174**: 838–39.
5 Read DH, Harrington DD, Keenan TW, Hinsman EJ (1976) *Science* **194**: 442–45.
6 Prieur DJ, Aherm-Rindell AJ, Murnane RD (1991) *Am J Pathol* **139**: 1511–13.
7 Donnelly WJ, Sheahan BJ, Rogers TA (1973) *J Pathol* **111**: 173–79.
8 Capecchi MR (1989) *Science* **244**: 1288–92.
9 Yagi T, Tokunaga T, Furuta Y, Nada S, Yoshida M, Tsukada T, Saga Y, Takeda M, Ikawa Y, Aizawa S (1993) *Anal Biochem* **214**: 70–76.
10 Yagi T, Nada S, Watanabe N, Tamemoto H, Kohmura N, Ikawa Y, Aizawa S (1993) *Anal Biochem* **214**: 77–86.
11 Nanba E, Suzuki K (1991) *Biochem Biophys Res Comm* **178**: 158–64.
12 Robertson EJ (1987) In *Teratocarcinomas and Embryonic Stem Cells: A Practical Approach* (Rickwood D, Hames BD, eds) pp 71–112. Oxford: IRL Press.
13 Williams RL, Hilton DJ, Pease S, Willson TA, Stewart CL, Gearing DP, Wagner EF, Metcalf D, Nicola NA, Gough NM (1988) *Nature* **336**: 684–87.
14 Thomas KR, Capecchi MR (1987) *Cell* **51**: 503–12.
15 Sakuraba H, Aoyagi T, Suzuki Y (1982) *Clin Chim Acta* **125**: 275–82.
16 Bradford MM (1976) *Anal Biochem* **72**: 248–54.
17 Folch J, Lees M, Stanley GHS (1957) *J Biol Chem* **226**: 497–509.
18 Williams MA, McCluer RH (1980) *J Neurochem* **35**: 266–69.
19 Svennerholm L (1957) *Biochim Biophys Acta* **24**: 604–11.
20 Saito T, Hakomori S (1971) *J Lipid Res* **12**: 257–59.
21 Roe JH (1955) *J Biol Chem* **212**: 335–43.
22 Swell AC (1979) *Clin Chem Acta* **92**: 411–14.
23 Huang K-C, Sukegawa K, Orii T (1985) *Clin Chem Acta* **151**: 147–56.
24 Callahan JW, Wolfe LS (1970) *Biochim Biophys Acta* **215**: 527–43.
25 Matsuda J, Suzuki O, Oshima A, Ogura A, Naiki M, Suzuki Y (1997) *Brain Dev* **19**: 19–20.
26 Gonatas NK, Gonatas JJ (1965) *Neuropathol Exp Neurol* **24**: 318–40.
27 Felton J, Meisler M, Paigen K (1974) *J Biol Chem* **249**: 3267–72.
28 Seyfried TN, Glaser GH, Yu RK (1978) *J Neurochem* **31**: 21–27.
29 Suzuki K, Suzuki K, Kamoshita S (1969) *J Neuropath Exp Neurol* **28**: 25–73.
30 Sango K, Nakayama S, Hoffmann A, Okuda Y, Grinberg A, Westphal H, McDonald MP, Crawley JN, Sandhoff K, Suzuki K, Proia RL (1995) *Nature Genet* **11**: 170–76.
31 Riboni R, Caminiti A, Bassi R, Tettamanti G (1995) *J Neurochim* **64**: 451–54.
32 Venn G, Mason RM (1985) *Biochem J* **228**: 443–50.
33 Ng Ying Kin NMK, Wolfe LS (1975) *Biochem Biophys Res Comm* **66**: 123–30.

Received 4 December 1996, revised and accepted 25 December 1996